AFRL-RW-EG-TR-2011-052

THREE-DIMENSIONAL DYNAMIC LOADING OF SAND

J. P. BORG

Marquette University, Dept of Mechanical Engineering
1515 W. Wisconsin Blvd
Milwaukee, WI 53233

L. C. Chhabildas

Air Force Research Laboratory, Munitions Directorate
101 West Eglin Blvd, Suite 135
Eglin AFB, FL 32542

February 2011

FINAL REPORT

AIR FORCE RESEARCH LABORATORY
MUNITIONS DIRECTORATE

■ **Air Force Materiel Command**   ■ **United States Air Force**   ■ **Eglin Air Force Base, FL 32542**

NOTICE AND SIGNATURE PAGE

Using Government drawings, specifications, or other data included in this document for any purpose other than Government procurement does not in any way obligate the U.S. Government. The fact that the Government formulated or supplied the drawings, specifications, or other data does not license the holder or any other person or corporation; or convey any rights or permission to manufacture, use, or sell any patented invention that may relate to them.

Qualified requestors may obtain copies of this report from the Defense Technical Information Center (DTIC) <http://www.dtic.mil/dtic/index.html>.
.

AFRL-RW-EG-TR-2011-052 HAS BEEN REVIEWED AND IS APPROVED FOR PUBLICATION IN ACCORDANCE WITH ASSIGNED DISTRIBUTION STATEMENT.

FOR THE DIRECTOR:

  //ORIGINAL SIGNED//   //ORIGINAL SIGNED//
_____   _____
HOWARD G. WHITE, DR-IV   LALIT C. CHHABILDAS, ST
Technical Advisor, AFRL/RWM   Program Manager, AFRL/RW

//ORIGINAL SIGNED//
_____
MATTHEW J. MATYAC, DR-III
Technical Advisor, AFRL/RWMW

This report is published in the interest of scientific and technical information exchange, and its publication does not constitute the Government's approval or disapproval of its ideas or findings.

REPORT DOCUMENTATION PAGE

Public reporting burden for this collection of information is estimated to average 1 hour per response, including the time for reviewing instructions, searching existing data sources, gathering and maintaining the data needed, and completing and reviewing this collection of information. Send comments regarding this burden estimate or any other aspect of this collection of information, including suggestions for reducing this burden to Department of Defense, Washington Headquarters Services, Directorate for Information Operations and Reports (0704-0188), 1215 Jefferson Davis Highway, Suite 1204, Arlington, VA 22202-4302. Respondents should be aware that notwithstanding any other provision of law, no person shall be subject to any penalty for failing to comply with a collection of information if it does not display a currently valid OMB control number. **PLEASE DO NOT RETURN YOUR FORM TO THE ABOVE ADDRESS.**

1. REPORT DATE	2. REPORT TYPE	3. DATES COVERED *(From - To)*
Feb 2011	Final	May, 2009 - Feb, 2011

4. TITLE AND SUBTITLE	5a. CONTRACT NUMBER
Three-Dimensional Dynamic Loading of Sand	FA8651-09-1-0011

4. TITLE AND SUBTITLE

Three-Dimensional Dynamic Loading of Sand

5a. CONTRACT NUMBER
FA8651-09-1-0011

5b. GRANT NUMBER

5c. PROGRAM ELEMENT NUMBER
61120F

6. AUTHOR(S)
J.P. Borg

L.C. Chhabildas

5d. PROJECT NUMBER
2303

5e. TASK NUMBER
DW

5f. WORK UNIT NUMBER
97

7. PERFORMING ORGANIZATION NAMES AND ADDRESSES
Marquette University, Dept of Mechanical Engineering
1515 W. Wisconsin Blvd
Milwaukee, WI 53233
Air Force Research Laboratory, Munitions Directorate
101 W. Eglin Blvd, Suite 135
Eglin AFB, FL 32542

8. PERFORMING ORGANIZATION REPORT NUMBER

9. SPONSORING / MONITORING AGENCY NAME(S) AND ADDRESS(ES)
Air Force Research Laboratory, Munitions Directorate
AFRL/RW
101 West Eglin Boulevard
Eglin AFB, FL 32542-6810

10. SPONSOR/MONITOR'S ACRONYM(S)
AFRL-RW-EG

11. SPONSOR/MONITOR'S REPORT NUMBER(S)
AFRL-RW-EG-TR-2011-052

12. DISTRIBUTION / AVAILABILITY STATEMENT
DISTRIBUTION A: Approved for public release; distribution unlimited. Approval Confirmation #AAC/PA 96 ABW-2009-0334, dated 4 August, 2009.

13. SUPPLEMENTARY NOTES

14. ABSTRACT
   The objective of this work was to assess the ability of Eulerian hydrocode simulations to model the rapid compaction of loose dry granular sand at moderate strain-rates on the order of 10^3 s^{-1}. The simulated results are compared to data obtained from Hopkinson bar experiments. Sim ulations were conducted in two configurations: t hree-dimensional mesoscale simulations and one-dimensional continuum simulations with the inclusion of a porosity model. The goal of the simulations was not to reproduce the experimental results by adjusting material or model properties but rather determine a baseline mesoscale solution given bulk material properties of quartz. A n additional goal was to probe the param eter space to determine what phy sical mechanisms are most essential to reproducing expe rimental data. It was fo und that even at these relatively low strain rates, th e dynamic yield strength of the underlying material (quartz) had to be increased above the static strength yield strength of 40 MPa. In addition the inclusion of grain-on-grain stiction (friction) plays a major role in the compaction of sand at low strain rates.

15. SUBJECT TERMS
Eulerian hydrocode, granular sand, dynamic loading

16. SECURITY CLASSIFICATION OF: UNCLASSIFIED			17. LIMITATION OF ABSTRACT	18. NUMBER OF PAGES	19a. NAME OF RESPONSIBLE PERSON
a. REPORT	**b. ABSTRACT**	**c. THIS PAGE**	SAR	17	1Lt Christopher Vineski
UNCLASSIFIED	UNCLASSIFIED	UNCLASSIFIED			**19b. TELEPHONE NUMBER** *(include area code)* 850-882-1812

Table of Contents:

List of Figures:

List of Tables:

Introduction

The dynamic compaction of loose dry granular material is fundamentally a multi-scale problem. Many engineering problems involving rapid l oading conditions exist at the bulk scale, and exam ples include planetary impact and crater formation, tectonic plate movement, ballistic im pact and penetration events. On a bulk scale, which includes t housands of grains of sand, the material behaves somewhat like a homogeneous hydrodynamic continuum. However as the charact eristic dimension of the analysis is reduced, the do minant phenomenological behavior is altered. At smaller scales, on the order to tens of grains of sand, the material form s heterogeneous structure, such as stress bridgin g, which serves to distribute loads. The result is a co mplicated stress field where grains within a bridge network carry nearly all of the load and grains outside of a bridge network carry nearly no load. At yet smaller scale, on the order of the grain contact surface, the material contact tensor determines the transmittal of stress from one grain to the next. At even smaller scale (those less than the grain itself) the non-isotropic material rheolog y behavior, such as grain y ield and defo rmation, plasticity and twinning, establish the dominant phenomenological behavior characteristics. Phenomenology at all of these scales feeds back to the bulk scale and ultimately dictates the response of the overall bulk system. However it r emains unclear as to whic h mechanisms dominate and which, if any, might therefore be neglected. The si mulations presented here resolve t he dynamic compaction behavior from the bulk scale (although not relative to most engineering systems) to the grain, but not sub-grain. At the scale of the grain and smaller the material is treated as a hom ogenous continuum solid. Thus t he term *meso* scale, which means middle scale, is used to describe the simulations presented here.

In addition to dynamics at multiple scales, the variability associated with loading rate can affect the dynamic response of materials. Quartz has famously demonstrated a rich variety of behaviors as a result of shock loading, including phase transitions, mat erial property variability as a function of driving pressure and sam ple thickness, as well as stress r elaxation effects [i-iv]. The strain rates under investigation here ($<10^3$ s^{-1}) are modest compared to shock loading ($10^5 \sim 10^6$ s^{-1}) but clearly in the dynamic regime. These loading rates ar e more characteristic of conditions found further way from an impact event, where the bulk material does not necessarily experience uniform loading in excess of the Hugoniot elastic li mit (HEL). An exam ple of such a loading condition is a t ransmitted stress wave emanating from a land mine explosion. The analysis is complicated by the heterogeneous nature of the material and therefore the loading. Although the bu lk stress state of the sand does not exceed the HEL, this does not imply that i ndividual grains won't exceed the HE L. The response of heterogeneous systems when subjected to these in termediate strain rates r emains of fundam ental importance in completing our understanding of the dynamic behavior of sand.

Thus, our aim is to explore the dy namic compaction of a heterogeneous sy stem using a mesoscale numeric approach at low to m oderate strain ra tes. Ultim ately it is hoped that these mesoscale simulations can be used to augmen t experimentation by exploring the state spa ce of a heter ogeneous system were experimental measurements are difficult or i mpossible, and serve as a platform by which continuum models can be developed or refined.

Background

Due to the computational expense associated with resolving a mesoscale simulation, the usefulness as applied to large sc ale engineering systems remains limited. Thus the need for continu um modeling persists. The variation in materi al properties associated with hete rogeneous systems, the inclusion of void space and void collapse, coupled with the lack of adequate experimental techniques to probe t he heterogeneous state, make continuum modeling challenging. Usually, granula r materials are modeled as a continuum (i.e. the grains and porosity are treated as a n ew single material) and a re assigned average properties. In so doing the heterogeneous nature of the material and the grain interactions are lost. In these continuum approaches additional constitutive relations such as the sphere collapse models [v], snowplow [vi], P-α [ϖιι], P-λ [ϖιιι] or $\sum$-alpha [ix] models are used to govern the removal of porosity.

Developments in com puter architecture and soph istication in par allelization have allowed large-scale simulations to explore multi scale pheno mena. A host o f researchers, utilizing a variety of numeric formulations such as Eulerian h ydrocodes, finite element or discrete elem ent methods, have successfully used mesoscale simulations to m odel many types of high rat e dynamic phenomena involving heterogeneous materials, including the shock compaction of elemental metals and alloys, the behavior of energetic materials, ceramic alloys and earth materials such as sand [x,xi,xii]. These studies have demonstrated that mesoscale simulations can be used to s uccessfully describe the high rate compaction dynamics without the use of additional constitutive relations, thus corroborating predictions from various analy tic porous collapse m odels and experimental observations [xiii,xiv,xv]. In most of these studies the focus was to num erically predict the bul k material behavior at high strain rates, i.e. Hugoniot behavior. It was shown that si mple formulations and simple descriptions on a grain level can combine to resolve complicated dynamics observed on the bulk scale such as the formation o f dynamic force chains, void collapse, turbulent like behavior and hot spot formation. This study differs from these in that we aim to explore the dynamic compaction at much lower strain rates, near 10^3 s^{-1}.

Experimental Data

The experimental data, which is compared to the simulations presented he re, was obtained from a split-Hopkinson pressure bar [xvi-xix]. The material used in these experimental investigations wa s silica based, kiln dried fine grai n sand. The particle size distribution was between 200-450 μm. The dynamic compressive response of t he sand was investigated at various moisture contents rangin g from 3% to 20% by weight with all specimens having a dr y density of 1.50 g/cm^3. The specimens were confined using a hard ened 4340 s teel tube with an outer diameter of 25.4 mm, inner diameter of 1 9.1 mm and length o f 50.8 mm . The steel tube is used to achieve high confinement pressures and to replicate a uni-axial st rain condition. The incident bar was
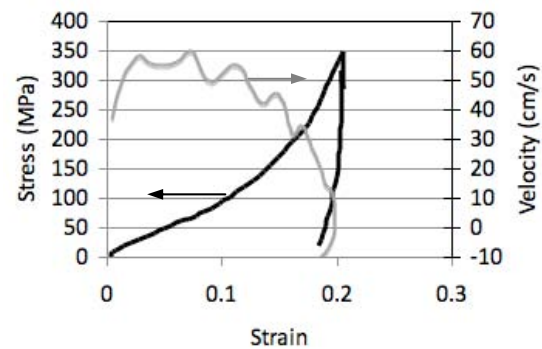
Figure 1: Uni-axial stress-strain behavior of sand, as well as the incident bar velocity, obtained from a split Hopkinson bar at a strain rate of 606 s-1 [16-18].

2

well controlled in or der to produce a near linear st rain (constant strain-rate of approxim ately 600 s^{-1}) over the test interval of 0.2 milliseconds. A r epresentative example of the r esulting axial stress data i s presented in Figure 1 as a function of strain. The reduction in stress at a strai n of approximately 0.2 represents significant unloading of the sample. The strain profile was differentiated in order to produce an incident bar velocity profile, also illustrated in Fi g. 1. This velocity profile was used as a boundar y condition for the simulations presented below.

Numeric Simulations

The simulations presented here were performed using the CTH hydrocode [xx]. The sand was modeled either as a collection of quartz spheres in a three-dimensional rectilinear dom ain for t he mesoscale simulations or as a single representative material in a one-dimensional domain for the continuum simulations. This was done so that the performance of each ty pe of si mulation could be assessed and compared. For both types of simulations, the motion of a rigid driver plate re presenting the incident bar was prescribed on the left side of the domain and a symmetry boundary condition was imposed on the right side of the domain to represent the longitudinal center of the sam ple. Figure 1 presents the velocity versus strain history that was used to prescribe the motion of the incident bar for these simulations. For the three-dimensional simulations, periodic boundary conditions were i mposed in the lateral direction. Greater detail regarding each type of simulation is presented below.

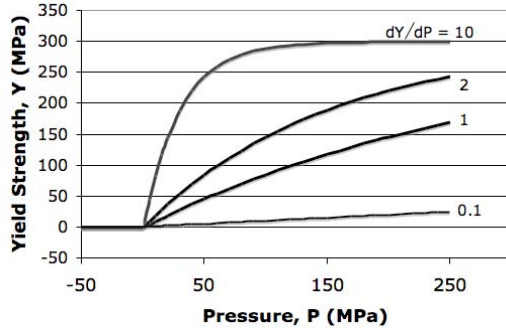*One-Dimensional Continuum Calculations*

Of fundamental importance when conducting contin uum simulations of heterogeneous materials is selecting the right constitutive relations; in this wor k several were investigated, however onl y one is presented here: a tabular EOS (sesame table) with a P-α compaction model [vii,xxi,xxii]. This equation of state had been previously developed for simulations of buried la nd mine explosions. The amplitude and duration of trans mitted stress waves far fro m land mine explosions is si milar to t he loading conditions applied by the split Hopkinson bar. A su ite of sesame tables for vary ing soil moisture content has been included in the stan dard release of CTH since version 8.0. For the simulations presented here the eos7860 tabular sesame was used, which was formulated for 4% moisture and bulk SiO$_2$ sand, where the grain densit y is 2.65 g/cc and the bul k density is 1 .56 g/cc. The underlying reference curve for the construction of these tabl es was the shock Hugoniot for quartz measured by Wackerle [i]. Kerley suggested that the pore compaction pressure be approximate with:

$$P_s = (500\,MPa)e^{-19.2w},\qquad\qquad(1)$$

where w is t he moisture content of the sand [xxii]. Thus assuming 4% m oisture, we obtain a pore compaction pressure of 232 MPa, however it was found that a value of 1,440 MPa best fit the Hopkinson bar data. The bulk strength of t he sand was modeled with a pressure dependent geological yield surface (GEO), previ ously implemented in CTH [xxiii]. The formulation for this y ield surface is presented in Equation 2 and is illustrated in Fig. 2. Experimental data from buried land mine explosions suggest the yield-pressure correlation, *dY/dP*, is approxim ately 2 and would remain positive through compaction. The yield offset strength, *Y′*, is approximately 80 MPa, and the bulk, zero pressure, yield

3

strength, Y_0, should be between 100-300 kPa, [xxi,xxii,xxiv]. The remaining material properties   , obtained from a vari ety of sources [xxv-xxvii], are list ed in Table 1. Note that variations in the   bulk yield strength had little effect on the axial stress obtained given the loads far exceed these strengths.

$$Y = Y' + (Y_0 - Y')\exp\left[\frac{P}{Y_0 - Y'}\frac{dY}{dP}\right] \quad \begin{array}{l} \text{for } dY/dP > 0 \\ \text{and } P \geq 0 \end{array}$$

$$Y = \min\left\{Y', Y_0 + P\left|\frac{dY}{dP}\right|\right\} \quad \begin{array}{l} \text{for } dY/dP < 0 \\ \text{and } P \geq 0 \end{array}$$

$$Y = Y_0 \quad \text{for } P<0$$

(2)

Figure 2: Pressure dependent geological yield surface

Table 1: Baseline constitutive relation constants for the continuum simulations

Tabular Equation of State Parameters[a]	Value	Pressure Dependent Geological Yield Parameters[a]	Value
Bulk Density, ρ_{00} [g/cc]	1.56	Max. Strength, Y' [MPa]	300
Grain Density, ρ [g/cc]	2.56	Yield Surface Slope, dY/dP	2
Pore compaction pressure, P_s [MPa]	232	Yield strength at zero pressure, Y_0 [MPa]	0.3
Zero stress shock speed, c_0 [km/s]	5.99	Poisson ratio, ν	0.32
Hugoniot slope, s	2.345	Tensile strength, σ_s [GPa]	0.0001

[a] Kerley [xxi,xxii]
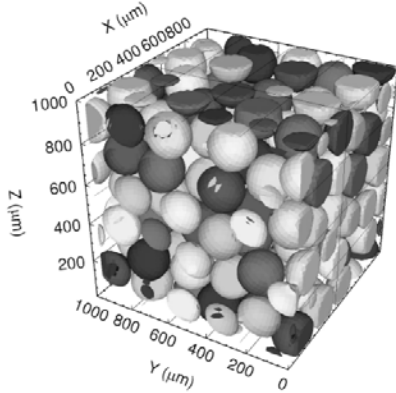
Three-Dimensional Mesoscale Calculations

The computational domain and m aterial properties utilized for the m esoscale simulations are presented in Fig. 3 and T able 2 respectivel y. Unlike the one-dimensional co ntinuum simulations, a mesoscale approach resolves the grain interaction directly, thus there is no need to approximate the bulk material properties or include a pore compaction model.

A Mie-Grüneisen equation of state (EOS) [xxviii]   with a perfectly elastic-plastic strength m odel was used to m odel each quartz sand grain. The EO S parameters are based on cry stalline quartz, i.e. silicon dioxide (SiO_2); the main constituent of Ottawa sand is 9 9.8% pure quartz [xxix]. Quartz has famously demonstrated a rich variety of behavior s as a result of shock loading, includ   ing phase transitions, material property variability as a function of driving pressure and sample thickness, as well as stress relaxation effects. Given the nature of the   Eulerian calculations, i.e. the inability to specify crystallographic orientation of indi vidual sand grai ns as well as the polycrystalline nature of grains, different bulk material properties are assigned to eac h sand grain. For exam ple, Table 2 list the shock Hugoniot properties of quartz as a function of t he orientation of the crystalline structure [ii]. However, instead of assigning averaged properties to all of the grains, we explore the effect of assigning the x-cut shock Hugoniot properties to half of th e grains in th e simulation and z-cut properties to the other half.

The effect of varying the material properties is not new to this work; a more detailed exploration of theses effects can be found in Branson, Wells and Strack [xxx] and Borg [xxxi]. The specific heat of quartz is reported between 0.74 J/g/K and 0.85 J/g/K [xxxii,xxxiii].

For these simulations, the grains behave elastically until the specified dynamic strength is achieved, at which point the material plastically flows. Estimates of the Hugoniot elastic limit (HEL) for the x- and y-cut axes are between 5.5 GPa to 8.5 GPa and 10 to 15 GPa for the z-cut axis, however hydrostatic data indicate the lower limit is closer to 2.3 GPa [i,iii]. Simulations were conducted in which the HEL for all the grains was varied from 2 to 12.4 GPa. The measured Poisson's ratio for quartz varies between 0.11~0.15, however it was set to 0.15 for these simulations [i].

The measured dynamic tensile strength, i.e. spall strength, of quartz exhibits variations with respect to loading conditions. Kanel *et. al.* report that the spall strength for x-cut quartz reaches 4 GPa for loadings below the HEL and falls to zero for loading conditions near the HEL [xxxiv]. The dynamic tensile strength is extremely high as compared to the static fracture of 44 MPa [xxxv]. The loss in spall strength is thought to result from accumulated damage, i.e. cracking of brittle single crystals under compression, ultimately resulting in a total loss of tensile strength near the HEL. Much like the shock Hugoniot parameters, and in order to understand the effect of strength on the bulk compaction, a range of spall strengths were assigned to the grains within a given simulation. Simulations were carried out where the tensile strength was varied from pre-damaged or static fracture strengths, near zero, to 4 GPa.

Figure 3: Three dimensional view of mesoscale geometry. Variations in gray scale are for visualization purposes only

Table 2: Baseline material and constitutive constants for the mesoscale simulations

Parameter	Quartz
Density, ρ [g/cm^3]	2.65
Zero stress shock speed, C_0 [km/s]	
x-cut	5.610
z-cut	6.329
Hugoniot slope, s	
x-cut	1.07
z-cut	1.56
Grüneisen coefficient, $\Gamma=V(\partial P/\partial E)_V$	0.9
Specific heat, C_V [$J/(g\text{-}K)$]	0.85
Bulk dynamic yield strength, Y [GPa]	
x-cut (low, average, high)	4.1, 5.8, 7.0
z-cut (low, average, high)	8.2, 10.3, 12.4
Poisson's ratio, ν	0.15
Fracture strength, σ_s [GPa	0.044 - 15 GPa

Given experimental observations that friction, be it grain-on-grain or between the sand and test fixture, has a significant effect on the resulting stress-strain behavior, we included some form of friction in the mesoscale simulation. Given the Eulerian nature of CTH, imposing a complete contact stress tensor on the surface of each grain would be difficult at best. However, CTH does allow the user to specify how the strength of a mixed material cells is calculated. When setting up the computational domains, care was taken to assign adjacent grains a different material number, thus enabling some control over the grain contact strength in mixed (i.e. touching) cells. We explored the effects of mixed cells being assigned either zero or the volume fraction averaged bulk yield strength: sliding or stiction

5

respectively. Sliding m eans there is no strength between materials in m ixed cells, where as stiction means that the initial grain network is welded. In either case, once the stress in a given cell exceeds the assigned strength, the material flows at the specified yield stress.

In previous high strain rate studies, 10^6 s^{-1}, conducted by the authors it has been found t hat mesh convergence is achieved for 10 com putational cells per grain per spatial direction. In this st udy, where the strain rates are much lower, the mesh was such that 20 cells per grain were needed. Given these requirements and the three-dimensional nature of the domain, the simulations required approximately 100 hours utilizing 64 pr ocessors, whereas the one -dimensional simulations required 15 minutes utilizing a single processor. One can see the value of further developing continuum level simulations.

Results

Mesoscale Simulation Results

In order to e xplore the mesoscal e results, the longit udinal stress, σ_{xx}, was averaged in the lateral direction for a given longitudinal position. The results are presented in Fig. 4 at two different snapshots in time, which translates to 19 and 31% strain, for both the stiction and sliding grain conditions. The simulations indicate that sliding results in substantia lly softer bulk stress as compared to s tiction. A particular feature of these relatively slow strain rate events is that the stress state is fairly constant ahead of the incide nt bar (dri ver plate). The transmittal of information occurs at a rate, on the order of the sound speed of quartz (6, 000 m/s) or possibly as slow as the sound speed o f bulk sand (~100 m/s), either of which is much faster than that of the dr iver plate (~1 m/s). In the context of a hy drocode written specifically to resolve wave phenom ena this translates into hundreds of stress r everberations between the sample thickness. Thus as the driver plate co mpacts the s and at relatively constant velocity, a time varying (strain varying) stress-strain state is achieved within the sand.

These results provide a justification to average the entire stress state of the sand in order to obtain a bulk axial stress state for a given displacement, i.e. strain. The results, presented in Fig. 5, indicate that the sand with sliding grain contact requires very little applied stress to strain to nearly 25% as compared to the grains with stiction. The simulations indi cate that the bulk com paction *snow plows* in its response, i.e. significant pore removal for little to no applied stress, before the bulk response stiffens. It is interesting to note that the maximum pack density of a monodisperse collection of spheres is $\pi/\sqrt{18}$ or 74%. Thus grain packing without friction slides t ogether rather unim peded until it is mechanically locks at near 25% strain, at which point the response stiffens. This behavior is illustrated in Fig. 5.

There are two modes in which grain material can be rearrange: 1) centroid motion, i.e. the grains moving without deforming and 2) grain deformation, i.e. a grain being deformed into a g ap. For both the sliding and stiction simulations m aterial is rearranged through a combination processes 1) and 2). The stiction simulations appear to have less c entroid motion and more grain deformation as compared to the sliding simulation. The sliding simulations do not achieve a face center ed cubic arrangement, i.e. maximum pack density. These assessments are purely qualitative; it is difficu lt to quantify how much of the material rearrangement is due to deformation and how much is due to centroid rearrangement.

6
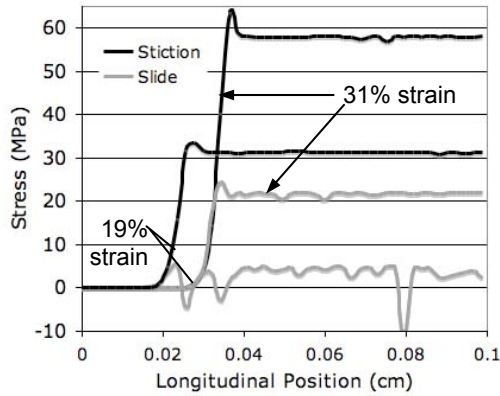
**Figure 4: Average longitudinal stress for grains with either stiction or sliding at two different strains**
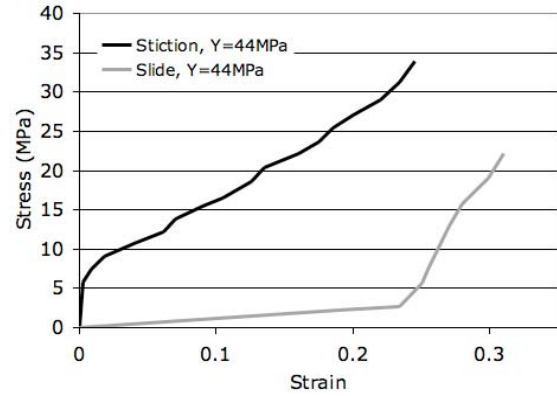
Figure 5 Stress-strain behavior for various grain and strength configurations

When compared to experimental stre ss-strain data, both t he stiction and slidi ng grain con ditions under predict the experimental behavior. Thus the average dynamic yield strength was increased by an order of magnitude, from 44 MPa to 440 MPa, to assess the effects on the bulk response; the results are presented in Fig. 6 along with experimental results for comparison. The results indicate an increase in the dynamic yield strength, over that of the st atic yield strength, is necessary to repr oduce the experimental results. Since the sliding grain co nditions indicated near sn owplow like behavior, whereas the data did not, sliding simulations with higher yield strengths are not presented.
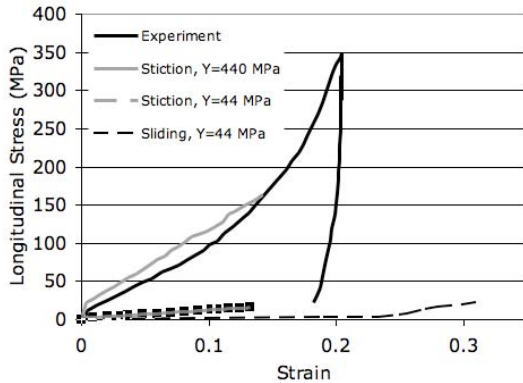
Figure 6: Bulk stress-strain for the mesoscale simulations as a function of grain boundary and dynamic yield strength
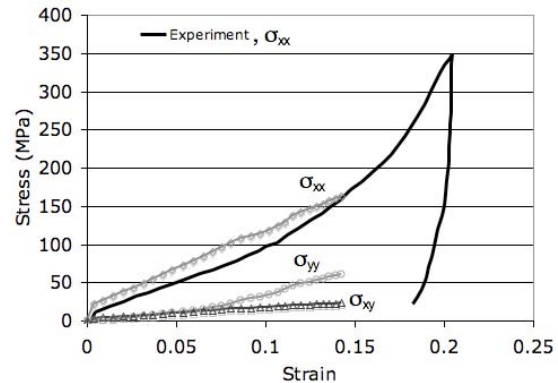
Figure 7: Stress tensor components for the mesoscale simulations with a dynamic yield strength of 440 MPa and stiction grain

In order to gain a better appreciat ion for th e complete stress stat e achieved within the heterogeneous system both the averaged lateral str ess and the averaged absolute value of the shear stress were computed from the mesoscale simulations and the results are presented in Fig. 7. Since the

7

average shear stress is zero; the absolute value of the shear stress was computed to gain an appreciation for amplitude of the relative shear compared to the longitudinal and lateral stress.

<div align="center">(a)   (b)   (c)</div>
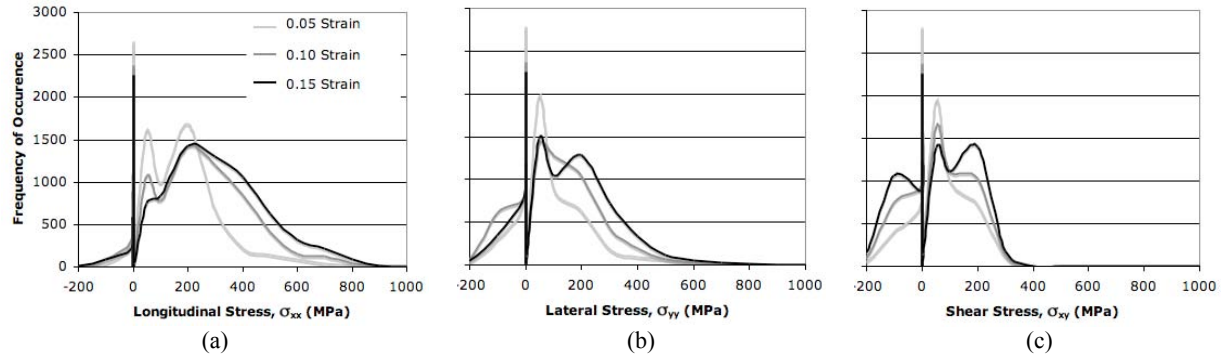
Figure 8: Stress distribution of averaged longitudinal, lateral and shear stress at 0.05, 0.1 and 0.15 strain

In order to better chara cterize the state of stress within the sand mixture, stress distributions were obtained from the mesoscale data. Figure 7 presents the distribution of the various tensor components of stress for all the com putational cells within the s imulation, at three different strains. The resulting distributions are non-normal (i.e. non-Gaussian). There are a large number of computational cells that experience no applied stress; thes e are represented as a large fr equency of oc currence at zero. As a result, the most probable occurrence of stress, i.e. the average str ess, does not appear centered on the distribution. For exa mple, at 0.15 strain Fi g. 7 indicates the average longitudinal stress, σ_{xx}, is approximately 160 MPa, which appear s lower than the peak occ urrence of stress presented in Fig. 8a for a strain of 0.15. In add ition there are relatively high stress *hot spots* experienced within the sand which are not completely characterized by the average, i.e. some computational cells are experiencing stress nearly an order of magnitude higher than th e average. Insights such as these, which are obtained from mesoscale simulations, could provide the way forward in our understanding of rapidly compacted heterogeneous systems, including both theoretical development and suggested experimental validation.

One-dimensional Simulation Results

Figure 9 presents the stress strain results from the one-dimensional simulations described above. Like the three-dimensional simulations, the one-dimen sional simulations with the original param eters under predict the dy namic response of the sand. By increasing the stress at which all of the pores ar e removed (i.e. the stre ss at which the P-α curve intersects the quartz Hugoniot) from 440 MPa to 1440 MPa, the sim ulations more accurately follow the experimentally measured material response. This modification of the baseline one-dimensional material parameters is not in complete agreement with the three-dimensional mesoscale simulations. In the mesoscale simulations the co mplete removal of porosity corresponds to t he intersection of the bulk dynamic response and the underl ying material Hugoniot, which is near the dynam ic strength assigned to the underlying material, i.e. 440 MPa. Thus the one-dimensional simulations require additional considerations.
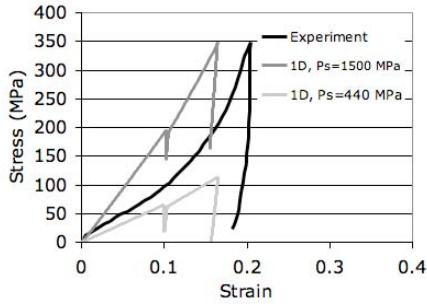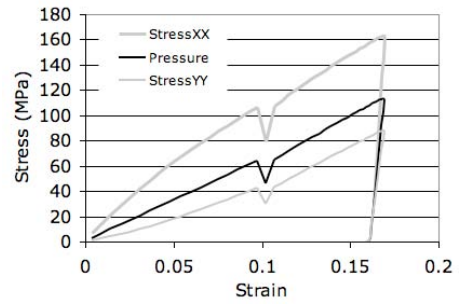
<div align="center">8</div>

Figure 9: Bulk stress-strain curve for the continuum simulations yield strength with varying pore compaction strength

Figure 10: Stress tensor components for the continuum simulations with a pore compaction strength of 1500 MPa

Discussion

One unanticipated aspect of this work was th e higher resol ution required to co nverge the simulation, which is nearly twice that of prev ious higher strain rate mesoscale simulations [xii]. I n general it is accepted that resolving each grain with 10 computational cells per grain, per axial direction is sufficient. However t hese lower s train rate si mulations demonstrated significant variations in response up to 20 cells per grain per axial direction. This could be a result of the high num ber of iterations required to ru n the simulation out to nearly 6 ms and the advection problems as sociated with the large number of iteration performed in Eulerian simulations.

For the simulations presented here, a distribution of yield and fracture strength was applied to the grain network in order to acce ss the e ffect on the bulk response. When appl ying a distribution of strength the key consideration is the average value. For the loading confi gurations investigated here, and the distribution of yield strengths from, 2 to 12.5 GPa, it was found that if the average did not vary then the bulk response did not var y. This is not the case for higher strain rat e investigations, 10^6 s^{-1} [xxxi]. In the higher strain rate studies it was f ound that an un derlying skeletal network of higher strength grains can form a percolated stress bridge which can stiffen the bulk response, this is especially true for stress levels near full compaction. For the lower strain rate studies conducted here, no such phenomena occurred. We are not sure if this is due to the allowable time for rearrangement, the low stress levels induced or the relatively narrow range of yield strength prescribed. Simulations presented here were sensitive to the variations in fracture strength, however. Vary ing the distribution of fracture strength could alter the bulk response of the grain network, even though the average value remained the same. This i s especially true if one ap plies a dram atic distribution of fracture strengths, i.e. half th e grains having a fracture strength of zero and half the grains having a fracture strength nea r the HEL. These results require further investigation.

The data presented in Fig. 7 is re-plotted in Fig. 11 a long with two-dimensional mesoscale results from high strain rate sim ulations and a ccompanying experiments, shown as open circles a nd dashed lines respectively [x,xxxvi]. It i s interesting to note that at higher strain rates, 10^6 s^{-1}, the presence of stiction over predicts the stiffness of the response as co mpared to experim ental data [x,xxxvi]. It is important to keep in mind that the high strain rate experimental data was obtained from a one-dimensional flyer plate experiment, whereas the data presented above was obtained from a Hopkinson

bar. The mesoscale simulations are nearly identical except they are at higher incident bar velocities and two-dimensional.
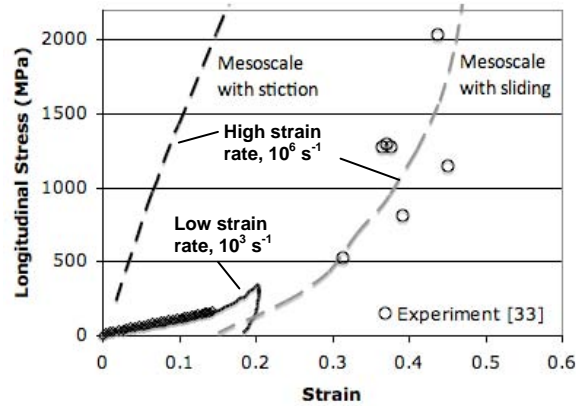
Figure 11: A comparison of high, 106 s-1, and low, 103 s-1, strain rate data and simulation. Low strain rate data from Fig. 7. High strain rate data, open circles, and accompanying mesoscale simulations, dashed lines, with stiction or sliding [10,36]

As Fig. 11 indicates, the sliding boundary condition better represents the ex perimentally determined dynamic response of the materi al at h igher strain rate. Both high and low strain rate simulations suggest that grain contact interactions can have a significant effect on the bulk response of the heterogeneous material but that the relevant contrib ution of friction varies as the strain rate varies, i.e. friction is important at low strain rat es, with dimensioning importance at higher strain rates. Explorin g these effects will continue for future studies.

Conclusions

Mesoscale simulations, such as those presented here, provide a rich backdrop for the exploration of rapidly compacted heterogeneous sy stems. Mesoscale simulations, which are a fairly new idea within the computational community, have yet to realize their full potential as a research tool in conjunction with experimental techniques, theoretical developm ent and/or continuum simulations. The simulations presented here indicate that low strain rate Eulerian mesoscale simulations require fairly high resolution to accurately predict the averaged longitudinal stress of a dynamically compacted sand sam ple. In addition, the simulations required that t he dynamic strength be an order of m agnitude higher than the static yield strength. The simulations further indicate that the presence of stiction (friction) is necessary to accurately predict the st ress-strain behavior as compared to experimental data. From the simulations a complete description of the averaged stress state, the longitudinal, lateral and shear stress, can be obtained. In addition, the simulations also indicate that this stress state is non-normal distributed within the sand sample and hot spots of stress can exists which are nearly ten times that of the av erage axial stress measured by the experiment.

References

[i]   Wackerle, J. *J. Appl. Phys.*, 33 (3), 922-937. 1962.
[ii]   Anan'in, AV, Breusov, ON, Dremin, AN, Persh in, SV and Tatsii, VF. *Combust. Explo. Shock*, 10 (3), (1974), 372-379.
[iii]   Fowles, R., *J. Geophys. Res.*, 72(22) (1967), 5729.
[iv]   Turin, RF. Shock Compression of Condensed Materials, Cambridge Press , 1998.
[v]   Carroll, M.M and Holt, A.C, Static and dynamic pore-collapse relations for ductile porous materials. Journal of Applied Physics. 43 1626-1636, 1972
[vi]   Asay, J.R. and Shahinpoor M., *High-Pressure Shock Compression of Solids*, Springer-Verlag, 1993, pg 7
[vii]   Hermann, W. Constitutive equation for the dynamic compaction of ductile porous materials, Journal of Applied Physics, 40 (6) , 2490-2499, 1969
[viii] Grady D.E. and Winfree N.A. (2001). A computational model for polyurethane foam, In K. P. Staudhammer, L.E. Murr, and M.A. Meyers, editors, *Fundamental issues and applications of shock-wave and high-strain-rate phenomena, Proceedings of EXPLOMET*, pages 485–491.
[ix]   Wunnemann K., Collins G.S., Melosh H.J. Icarus 180, 514-527, 2006
[x]   Borg, J.P. and Vogler, T.J., The Effect of Water Content on the Shock Compaction of Sand in Proceedings of the Dynamic Behavior of Materials, DYMAT 2009 Brussels Belgium, pg 1545–1551
[xi]   Crawford, D.A. 2005. Using mesoscale modeling to investigate the role of material heterogeneity in geologic and planetary materials. In: Shock compression of Condensed Matter – 2005, pp. 1453-1457.
[xii]   Borg, J.P. and Vogler, T .J., Mesoscale calculations of the dynam ic behavior of a gra nular ceramic *Int. J. Solids Struct.* 45, 1676–1696, 2008
[xiii] Benson, D.J., Nesteren ko, V.F., Jonsdottir, F.F. an d Meyers, M.A.   Quasistatic and dynamic regimes of granular matrial deformation under impulse loading *J. Mech. Phys. Solids,* **45**(11) 1955-1999, 1997
[xiv]   Nesterenko, V.F., *Dynamics of Heterogeneous Materials*. Springer, 2001
[xv]   Tong, W, Ravichandran, F., Christman, T. and Vreeland T., 1995. Acta Materialia 43, 230-250.
[xvi]   Martin, B.E., Chen, W., Song, B., Akers, S.A., "Moisture effects on the high strain-rate behavior of sand" Mechanics of Materials (in press)
[xvii]   Martin, B.E., and Chen, W. "The High-Rate Behavior of a Fine Grain Sand" Proceedings of the SEM Annual Conference, June 1-4, 2009 Albuquerque New Mexico USA
[xviii]   Martin, B.E., and Chen, W. "Response of Moist Sand to High Rate Loading" Proceedings of the DYMAT 2009, EDP Sciences, 201–205, 2009, Brussels Belgium
[xix]   Bragov, AM, Kotov, VL, Lomunov, AK, and Sergeichev, IV, "Measurement of the Dynamic Characteristics of Soft Soils Using the Kolsky Method". J. Appl. Mech. Tech. Phys., 45(4), 580-585, 2004
[xx]   McGlaun, J. M. Thompson, S. L. and Elrick, M. G., "CTH: a T hree-Dimensional Shock Wave Physics Code," *Int. J. Impact Engng.*, **10**, 351-360, 1990.
[xxi]   Kerley, GI, The Effects of Soil Type on Numerical Simulations of Buried Mine Explosions, Kerley Technical Services report KTS02-3, August 2002.
[xxii] Kerley, G.I., On the Numerical Simulation of Buried Mine Explosions: Choosing Constitutive Models. Kerley Technical Services, KTS05-3, Aug. 2005

[xxiii]   Crawford, DA, Bell, RL, Brundage, AL, Bruner, CW, Elrick, MG, Hertel, ES, Schmitt, RG, Schumacher, SC, Silling, SA, Simmons JS and Taylor, PA. CTH User's Manual and Input Instructions Version 8.1, Nov. 2007

[xxiv]   Windham, J., U. S. Army Engineer Research and Development Center, Waterways Experiment Station, Vicksburg, MS, private communication.

[xxv] Velea, D. S hields, FD a nd Sabatier JM. "Elastic   wave velocities in partially satu   rated Ottawa sand: experimental results and modeling" *Soil Sci. Soc. Am. J.* 64, 1226–1234, 2000.

[xxvi]   Verma, DK and Shaw, DS. "A comparison of international silica (α-quartz) calibration standards by fourier transform–infrared spectrophotometry" *Ann. Occup. Hyg.*, 45(6), 429–435, 2001.

[xxvii]   Hertel, ES and Kerley, GI. "CTH EOS package: introductory tutorial", Sandia Report 98-0945, 1998.

[xxviii]   Rice, MH, McQueen, R.G. and Walsh, J.M. "Compression of Solids by Strong Shock Waves" *Solid State Phys.* 6 (1), 1958.

[xxix]   American Society for Testing and Materials (ASTM) standard C-778

[xxx] Brannon, R. M., Wells, J., M., Strack, O.E., "Validating theories for brittle damage," Metallurgical and Materials Transactions A 38A, 2861-2868, 2007.

[xxxi]   Borg, JP and Vogler, TJ, "The Effect of Water Content on the Shock Compaction of Sand", in DYMAT 2009 - 9th International Conferences on the Mechanical and Physical Behaviour of Materials under Dynamic Loading, vol. , 2009, pp. , 1545-1552, published by EDP Sciences (www.dymat-proceedings.org).

[xxxii] Grady, D.E. *J. of Geophysical Research* 85, N. B2, (1980), 913-924.

[xxxiii] Schroeder, DV., An Introduction to Thermal Physics, Addison-Wesley, 2000.

[xxxiv] Kanel', Razorenov and Utkin, *High-Pressure Shock Compression of Solids II* edited by Davison, Grandy and Shahinpor, Springer (2004) pg 121

[xxxv] C.H. Scholz, *J. of Geophysical Research*, 77 (11), 1972

[xxxvi] Chapman, DJ, Tsembelis, K, Proud WG Proceedings of the 2006 SEM annual conference and exposition St. Louis, MO June 4-7 2006

DISTRIBUTION LIST
AFRL-RW-EG-TR-2011-052

Defense Technical Information Center   1 Electronic Copy (1 File & 1 Format)
Attn: Acquisition (OCA)
8725 John J. Kingman Road, Ste 0944
Ft Belvoir, VA 22060-6218

EGLIN AFB OFFICES:

AFRL/RWOC (STINFO Office)- 1 Hard (Color) Copy
AFRL/RW CA-N   - STINFO Officer Provides Notice of Publication
AFRL/RWME   -   1 Copy
AFRL/RWMF   - 1 Copy
AFRL/RWMW   - 1 Copy
AFRL/RWMI   - 1 Copy